August 2020 · Vol. 43 – No. 8
CETEER 43 (8) 2020 · 1463 – 1668 · ISSN 0930-4125

Chemical & Engineering Technology

Focus Issue: Bioenergy: The X-Factor
Guest Editors: Daniela Thrän and Diana Pfeiffer

8/2020
www.cet-journal.com
WILEY-VCH

Chemical Engineering and Technology

Country Germany - SIR Ranking of Germany

Subject Area and Category
Chemical Engineering
- Chemical Engineering (miscellaneous)

Chemistry
- Chemistry (miscellaneous)

Engineering
- Industrial and Manufacturing Engineering

Publisher Wiley-VCH Verlag

Publication type Journals

ISSN 09307516, 15214125

Coverage 1978, 1987-2020

75
H Index

Scope This is the journal for chemical engineers looking for first-hand information in all areas of chemical and process engineering. Chemical Engineering & Technology is: Competent with contributions written and refereed by outstanding professionals from around the world. Essential because it is an

Homepage

How to publish in this journal

Contact

Join the conversation about this journal

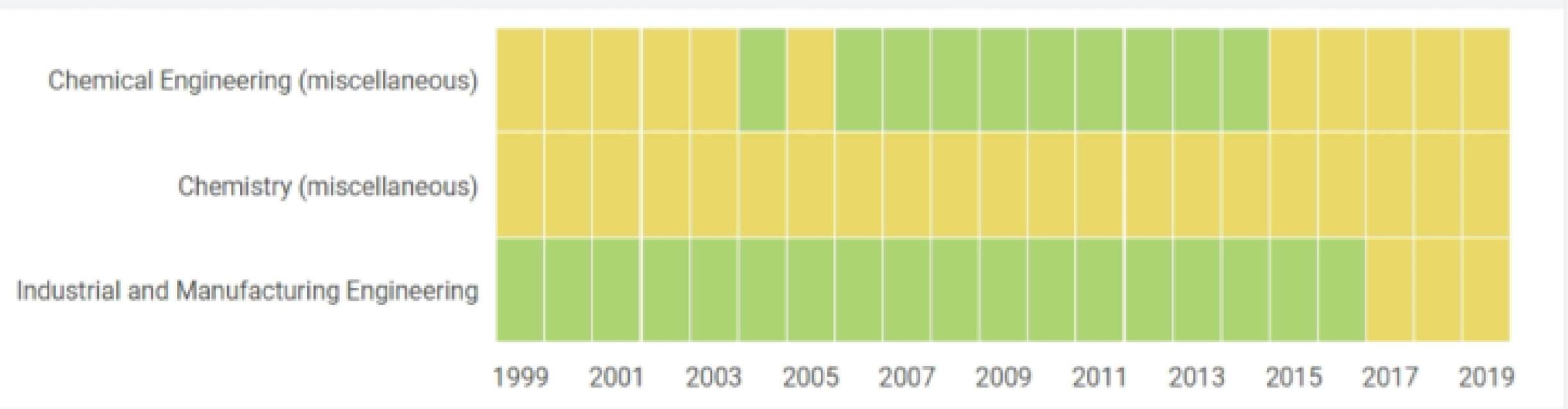

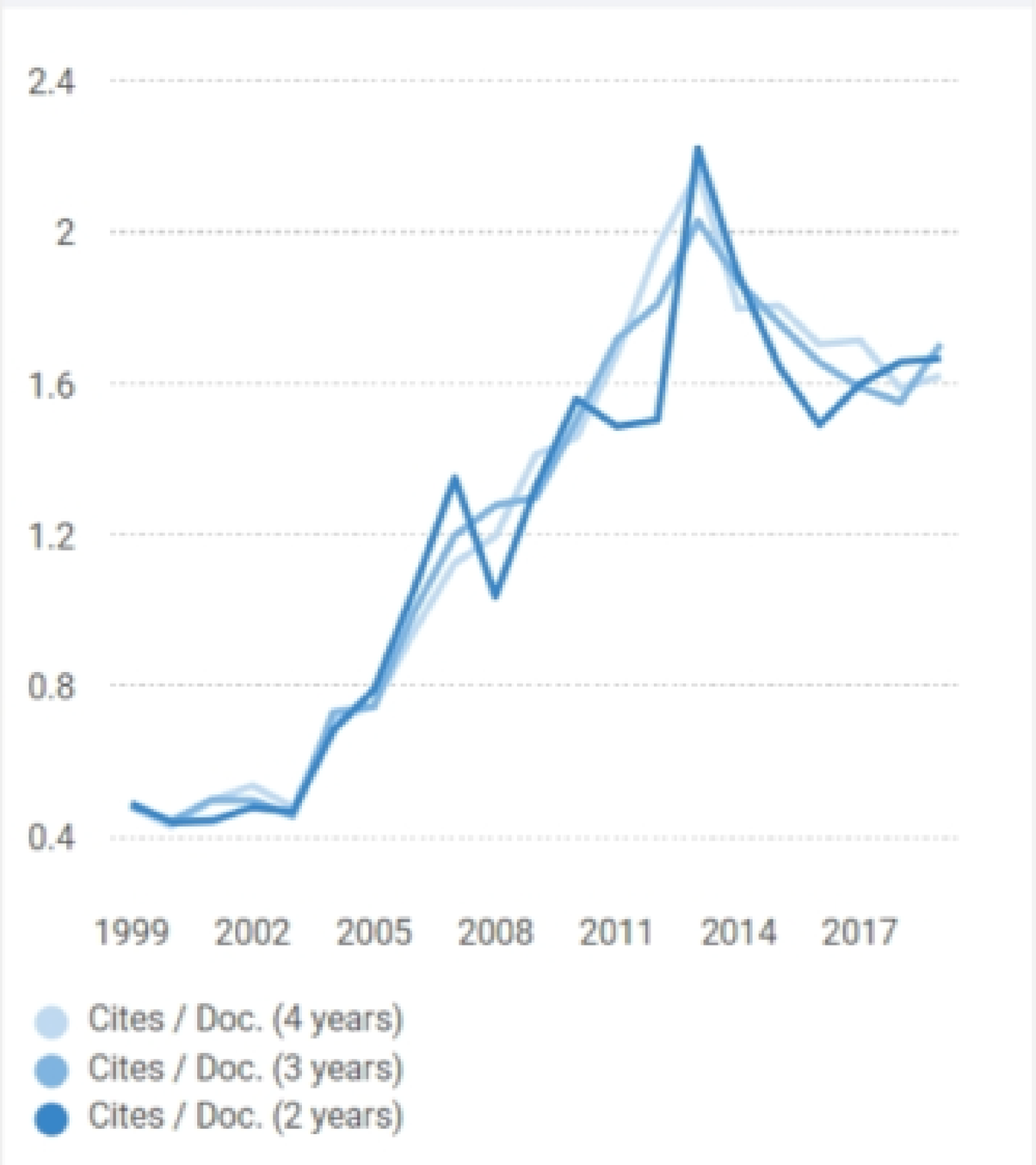

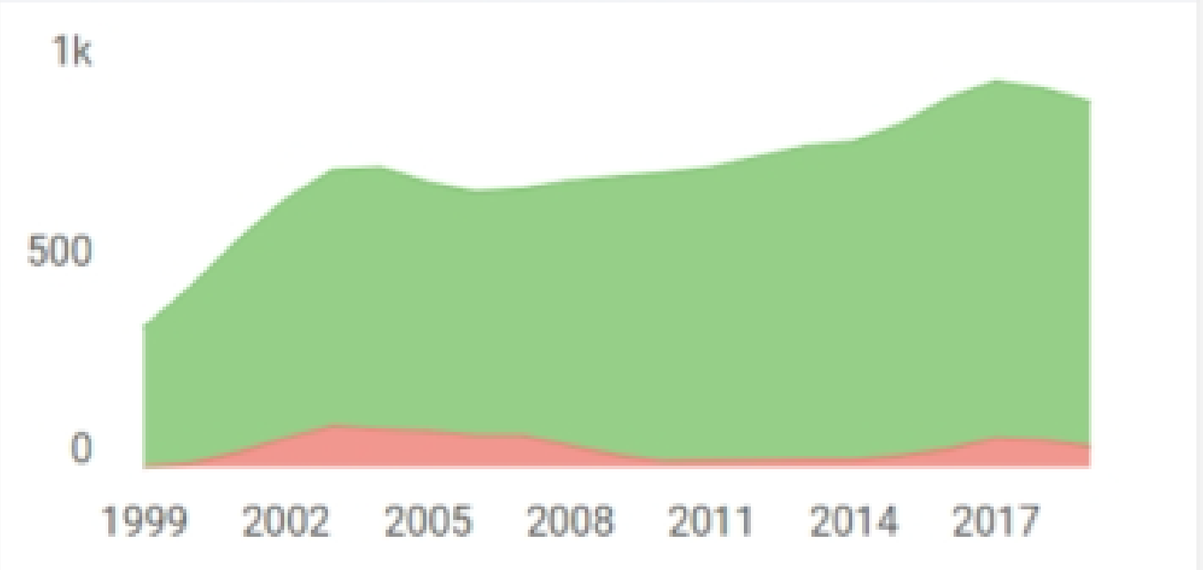

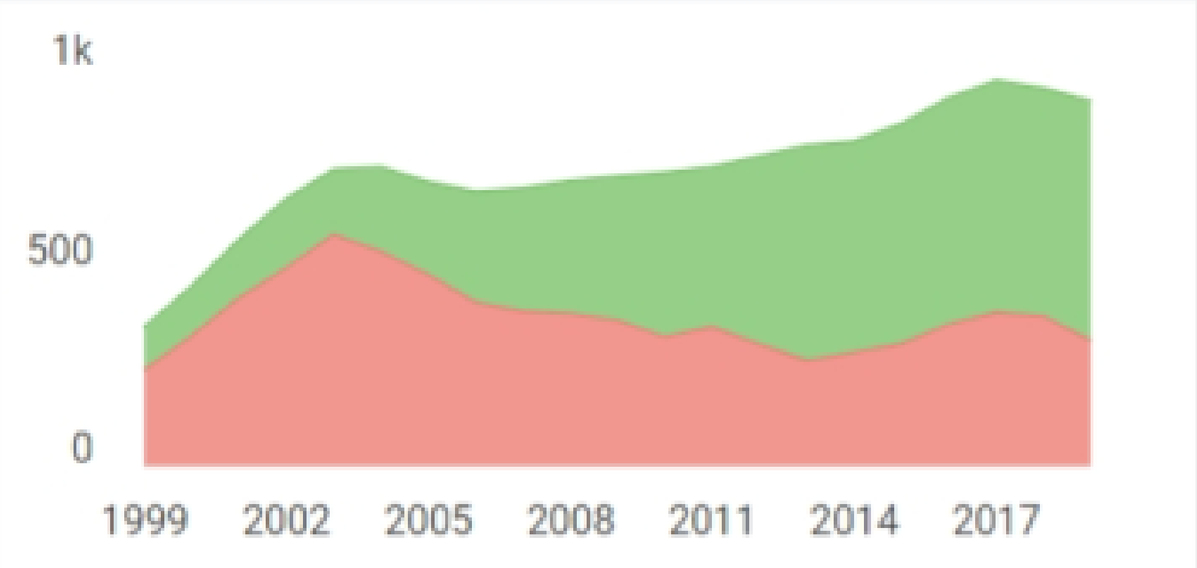

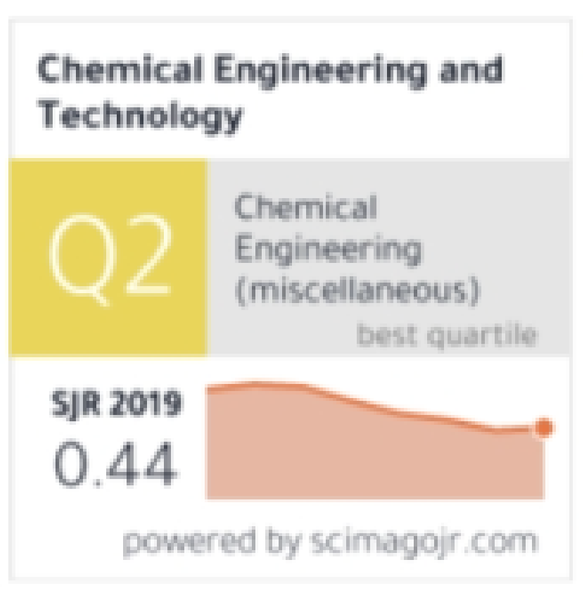

← Show this widget in your own website

Just copy the code below and paste within your html code:

<a href="https://www.scimag

Metrics based on Scopus® data as of April 2020

Georgian Technical University 7 months ago

We Greetings to you! wish you health and creative success!
The scientific group of the Engineering Institute of Membrane Technologies of the Georgian Technical University wants to cooperate with you and publish an article in the. Please write us all the necessary conditions for the publication of the article, price and send us an e-mail at mananamamula@gmail.com
Thank you in advance for your understanding.
Manana Mamulachvili, Research fellow at the Engineering Membrane Technology at Georgian Technical University

reply

Melanie Ortiz 7 months ago SCImago Team

Dear Sir/Madam,
thank you for contacting us.
We are sorry to tell you that SCImago Journal & Country Rank is not a journal. SJR is a portal with scientometric indicators of journals indexed in Elsevier/Scopus.
Unfortunately, we cannot help you with your request, we suggest you to visit the journal's homepage (See submission/author guidelines) or contact the journal's editorial staff , so they could inform you more deeply.
Best Regards, SCImago Team

Noraini Razali 2 years ago

Dear Publisher,
I am Noraini Razali, and currently a secretariat of Publication Unit in my institution.

Actually, my institution (Universiti Teknologi MARA) will organised a conference which will be held on March 2020.

The name of the conference is Terengganu Multidisciplinary International Conference (TEMIC 2020)

We are interested to publish the research paper in this jurnal.

May we know :-
1. how the process is?
2. Publication charges (if any) how much it cost for each article or per bulk of papers?
3. Publication time

Thanking you in advanced for your kind cooperation and hope to hear positively from you soon.

reply

mahmoud 2 years ago

In this study: with respect to the growing demand of the world, fossil sources, the need for renewable and renewable resources, It's morel need every day.
Scientific research on biofuels began in the late 1970 s and early 1980 s in the United States and Europe with the objective of production. In 1988, the first commercially viable product of biodiesel was produced from Rapeseed seed, and the first time in the United States was founded in 1992 by the American National Research Institute.
In other words, biodiesel is ethyl ester or methyl ester produced from vegetable oils or animal fats and used as fuel in diesel engines or thermal systems. Biodiesel can also be produced in addition to fresh oils ¹ (SVO), waste oils Â (WVO).
Different methods have been proposed in the world to produce biodiesel. The most important factors affecting the type of process are the type of feed used and the capacity of the process. The problem of reactive distillation can be studied using various methods, including feasibility, simulation, modeling, design and empirical studies in laboratory and pilot. A combination of these methods will provide the right solution. One of the most important aspects of predicting the behavior of these systems is the model used to design and simulate the process of reactive distillation.
The present work aims to find the more preferable reactive distillation and downstream separation process following a process simulation approach to obtain a pure biodiesel fuel 99 wt. %. The currently most efficient distillation models considered, i.e., alkali and heterogeneous catalysts, for biodiesel.
Productions were compared to determine the most cost-effective process. Pure soybean oil was used as process feedstock due to its low free fatty acids content (less than 0.3%); which prevents the need of a pre-treatment process. The two processes are compared based on a detailed economic analysis

reply

Leave a comment

Name

Email
(will not be published)

I'm not a robot
reCAPTCHA
Privacy - Terms

Submit

The users of Scimago Journal & Country Rank have the possibility to dialogue through comments linked to a specific journal. The purpose is to have a forum in which general doubts about the processes of publication in the journal, experiences and other issues derived from the publication of papers are resolved. For topics on particular articles, maintain the dialogue through the usual channels with your editor.

Chemical Engineering & Technology

Impact factor: 3.742
2019 Journal Citation Reports (Clarivate Analytics): 40/143 (Engineering, Chemical)
Online ISSN: 1521-4125

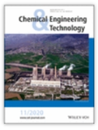

LATEST ISSUE >
Volume 43, Issue 11
November 2020

HOME | ABOUT | CONTRIBUTE | BROWSE

On the Cover

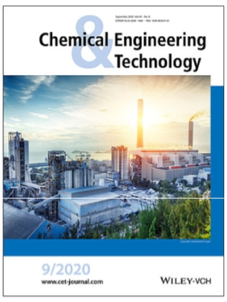

Glowing light of petrochemical industry at sunset. Copyright: cozyta@Getty Images

Play | Pause

MORE >

Articles

Most Recent | Most Cited

Characterization of New Wire Gauze-Structured Packing: Experimental Study

Tran Dinh Manh, Nguyen Dang Nam, Houman Babazadeh, Rasoul Moradi

First Published: 10 November 2020

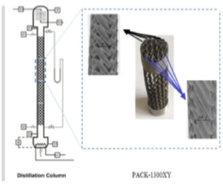

The performance of a new structured packing with wire gauze sheets, PACK-1300XY, with high porosity domain and specific surface area is experimentally studied in terms of height equivalent to a theoretical plate and wet and dry pressure drop in conflicting operating situations. This packing is applicable for distillation with high capacity, low pressure drop, and high mass transfer efficiency.

Abstract | Full text | PDF | References | Request permissions

Excellent CO_2 capture by ultra-high microporous activated carbon made out from Natural Coal

Ouassim Boujibar, Fouad Ghamouss, Arunabh Ghosh, Ouafae Achak, Tarik Chafik

First Published: 10 November 2020

Abstract | PDF

Characterization of New Structured Packing by using of computational fluid dynamics

Amin Hassanvand, Seyyed Hamid Esmaeili-Faraj, Mojtaba Saei Moghaddam, R. Moradi

First Published: 10 November 2020

Abstract | PDF

Heat Integration in Straight-through Sulfur Recovery Units to increase net High-Pressure Steam production

Anoop Jagannath, Salisu Ibrahim, Abhijeet Raj

First Published: 10 November 2020

Abstract | PDF

Degradation of atenolol in rectangular staircase photocatalytic reactor with immobilized ZnO

Madjene Farid, Assassi Mirvet, Yeddou-Mezenner Nacera

First Published: 3 November 2020

Abstract | PDF

MORE >

Recent issues

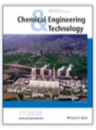

Volume 43, Issue 11
Pages: 2135-2344
November 2020

Volume 43, Issue 10
Pages: 1903-2134
October 2020

Volume 43, Issue 9
Pages: 1669-1902
September 2020

Volume 43, Issue 8
Bioenergy: The X-Factor
Pages: 1463-1668
August 2020
Issue Edited by:
Daniela Thrän,
Diana Pfeiffer

Submit a Manuscript
Browse free sample issue
Get content alerts
Subscribe to this journal

Supported by GDCh, VDI, Dechema

Citation Search

More from this journal

- News
- Topical Issues
- Editorials
- Portal: ChemistryViews
- Call for Papers

Virtual Issues

- CO_2 Capture
- Membrane Technology – Applications
- Membrane Technology – Syntheses and Modifications

ISSUE
Volume 92, Issue 11
Bioraffinerien
Pages: 1637-1859
November 2020
Issue Edited by:
Martin Bertau,
Roland Ulber

ISSUE
Volume 7, Issue 5
Pages: 147-166
October 2020

ISSUE
Volume 8, Issue 11
November 2020

WILEY

Chemical Engineering & Technology

Editorial Office

Chemical Engineering & Technology,
Wiley-VCH GmbH,
Boschstraße 12, D-69469 Weinheim,
Germany
Tel. (+49) 6201 606 520
Fax (+49) 6201 606 328
E-mail: cet@wiley.com

Advertising

Marion **Schulz**, Advertising,
Wiley-VCH GmbH,
Boschstraße 12, D-69469 Weinheim,
Germany
Tel. (+49) 6201 606 565
Fax (+49) 6201 606 551
E-mail: mschulz@wiley.com

Published monthly by Wiley-VCH GmbH,
D-69469 Weinheim, Germany.

Typeset by Kühn & Weyh Software GmbH,
Freiburg, Germany.
ISSN 1521-4125 (Online)

Supporting Organizations

- German Chemical Society (GDCh)
- Society for Chemical Engineering and Biotechnology (DECHEMA e.V.)
- Society for Chemical Engineering and Process Technology (VDI-GVC)

Abstracting and Indexing Information

- APILIT/American Petroleum Institute Literature (Elsevier)
- BIOBASE (Elsevier)
- CAB Abstracts®(CABI)
- Cambridge Scientific Abstracts (CIG)
- Chimica Database (Elsevier)
- Chemical Abstracts Service/SciFinder (ACS)
- COMPENDEX (Elsevier)
- Current Contents®/Engineering, Computing & Technology (Thomson ISI)
- FIZ Karlsruhe
- FLUIDEX (Elsevier)
- Science Citation Index® (Thomson ISI)
- Science Citation Index Expanded™ (Thomson ISI)
- SCOPUS (Elsevier)

For the USA and Canada: "Chemical Engineering and Technology". The identification statement should be corrected to read as follows: "Chemical Engineering and Technology" (ISSN 0930-7516) is published monthly by Wiley-VCH, PO Box 191161, D 69451 Weinheim, Germany. US mailing agent: Mercury Media Processing, LLC, 1850 Elizabeth Avenue, Suite #C, Rahway, NJ 07065 USA. Periodical postage paid at Rahway, NJ. POSTMASTER: send address changes to Chemical Engineering and Technology, John Wiley & Sons Inc., C/O The Sheridan Press, PO Box 465, Hanover, PA 17331

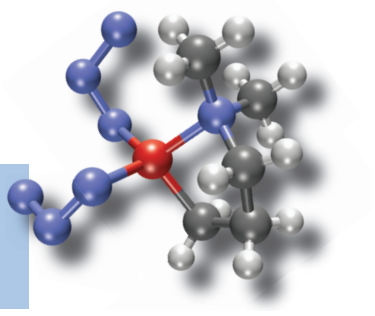

Homepage
www.cet-journal.com

Manuscript Submission
Online Submission of Manuscripts

Editorial

Bioenergy: The X-Factor

Daniela Thrän

Diana Pfeiffer

Following the title of this Special Issue "Bioenergy: The X-Factor" the X represents the multifaceted use of bioenergy in the various energy sectors, the flexibility from storage to power-to-X, the wide range of biomass and biogenic residues, the technology mix as well as the diverse and well networked stakeholders. Bioenergy is therefore a high potential partner in the future energy mix, providing missing components for 100 % renewable energy systems.

The manifold roles of bioenergy in future energy systems are also reflected in the articles in this issue. The presented technology and application developments show different smart and efficient options. They focus on the optimization of pretreatment and emission reduction strategies in biogas plants, small-scale gasification, gasification plants and furnaces as well as biorefineries. Looking from the user side, investigations deal with the status and perspectives of biomass use for industrial and heating sectors, demand-oriented power generation, marine fuel and renewable kerosene for mobility. In context of the current European and German Hydrogen Strategy the results on the production of biohydrogen from biomass and the synthesis of light hydrocarbons from biogas and hydrogen are particularly promising with respect to CO_2 neutrality. Furthermore, digitalization and flexibilization measures improve the integration of biogas plants, industrial biomass furnaces and hybrid plants in dedicated energy supply tasks.

The basis for smart bioenergy technologies and supply is in particular the sustainable provision of biomass to avoid new conflicts of use. Starting from the input stream, the considered biomasses increasingly include residual and especially waste materials. They cover a wide spectrum from wood chips, wheat straw, pig manure, and lignocellulose non-edible feedstocks to compost. This increases the challenge of adapting the processes and technologies for an optimized and efficient treatment of residual and waste materials. Finally, comprehensive assessment approaches for smart bioenergy systems can evaluate the potential of technologies and concepts also beyond the energy supply.

All this research efforts pursue the goal to fulfill the dimensions of the Sustainable Development Goals (SDGs). Bioenergy systems are becoming more and more efficient and sustainable and are increasingly better integrated into the renewable energy system.

In order to further expand the potential of bioenergy for efficient use and for the rapid transfer of research results into applications, the Federal Ministry of Economics and Energy (BMWi) is funding bioenergy projects under the funding area "3.7 Energetic use of biogenic residues and waste materials" via the 7th Energy Research Programme. Current research findings and challenges of the (bio)energy world were presented and discussed at the conference *Bioenergy: The X-Factor* in 2019 in Leipzig, Germany.

With the paper collection from this conference we hope to give you new insights into the latest research results for an optimized future bioenergy use in X dimensions.

Daniela Thrän
DBFZ Deutsches Biomasseforschungszentrum gGmbH, Head of Department of Bioenergy Systems;
Helmholtz Centre for Environmental Research – UFZ, Bioenergy Systems, University of Leipzig

Diana Pfeiffer
Department of Bioenergy Systems, DBFZ Deutsches Biomasseforschungszentrum gGmbH

Submit a Manuscript

Browse free sample issue

Get content alerts

Subscribe to this journal

More from this journal

- News
- Topical Issues
- Editorials
- Portal: ChemistryViews
- Call for Papers

Virtual Issues

- CO_2 Capture
- Membrane Technology – Applications
- Membrane Technology – Syntheses and Modifications

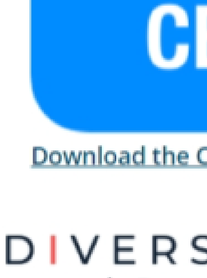

ISSUE
Volume 92, Issue 11
Bioraffinerien
Pages: 1637-1859
November 2020
Issue Edited by:
Martin Bertau,
Roland Ulber

ISSUE
Volume 7, Issue 5
Pages: 147-166
October 2020

ISSUE
Volume 8, Issue 11
November 2020

WILEY

ISSN 0930-4125, Volume 43, No. 8
August 2020, Pages 1463–1668

Home page: http://www.cet-journal.com
Full text: http://wileyonlinelibrary.com

Chemical & Engineering Technology

Editorial

Focus Articles

Research Articles

Jono Suhartono[1,*]
Dyah Setyo Pertiwi[1]
Carlina Noersalim[1]
Devi Yulianingsih[1]
Falashiva Sofianti[1]
Agus Saptoro[2]
Achmad Chafidz[3]

Characteristics and Performances of Blended Polyethersulfone and Carbon-Based Nanomaterial Membranes: Effect of Nanomaterial Types and Air Exposure

Polyethersulfone (PES) is a widely used polymeric material for ultrafiltration or nanofiltration membranes. To enhance membrane permeability, rejection, and antifouling performance, the effect of four different types of carbon-based nanomaterials and air exposures during PES/carbon-based nanomaterial membrane fabrication was evaluated. The carbon-based nanomaterials were pristine carbon nanotubes, oxidized CNTs (CNTs-O), pristine graphene nanoplatelets (GNPs-P), and oxidized graphene nanoplatelets (GNPs-O). The characteristics and performances of pure and blended membranes were investigated based on their permeability, porosity, morphology, and hydrophobicity. Longer air contact time during membrane preparation resulted in lower membrane permeability, hydrophobicity, and porosity. All fabricated membranes tended to have channelled sponge-like structure, and highest permeability was attributed to the PES/GNPs-O membrane.

Keywords: Carbon nanotubes, Graphene nanoplatelets, Impregnated polyethersulfone membrane, Polyethersulfone

Received: October 25, 2019; revised: March 22, 2020; accepted: April 24, 2020

DOI: 10.1002/ceat.201900582

1

The demand for fresh water is rapidly growing due to the steadily increasing world population. In this regard, membrane separation technologies including reverse osmosis, nanofiltration, ultrafiltration, microfiltration, membrane distillation, and pervaporation play essential roles in purification of natural waters and wastewaters for drinking water [1]. Membrane processes are favorable compared to other separation processes due to their low capital and operating costs, efficient energy requirement, and ease of operation [2, 3]. Consequently, research activities on membrane fabrication and how to further improve their separation performances have been a subject of interest in the past few decades.

Different types of materials have been adopted to fabricate membranes: polyvinylidene fluoride (PVDF), polyether sulfone (PES), polyacrylonitrile (PAN), polyvinyl alcohol (PVA), polyvinyl chloride (PVC), polyethylene poypropylene, polyamide. and chitosan [4]. Among the above, polyether sulfone (PES) is the most common material to manufacture membranes because of its superior thermal, mechanical, and chemical strengths [4–7]. Nevertheless, PES is acknowledged as a hydrophobic polymer which is easily able to absorb organic pollutants which cause membrane fouling [3, 8, 9]. This leads to decreasing membrane flux and higher maintenance and operation costs. Thus, it is desirable to modify PES membranes in order to minimize their hydrophobic properties. These modifications can usually be carried out through grafting [10, 11], coating [9, 12], or blending [9, 13, 14] to form impregnated membranes.

Various nanoparticles have been reported in the literature to be potential nanofiller materials for membrane impregnation. These nanofillers include oxide compounds such as TiO_2, Fe_3O_4, and SiO_2, metals including Ag and Cu, composites, metal-organic frameworks (MOFs), and carbon nanomaterials, e.g., carbon nanotubes and graphene [9, 15]. Among these nanomaterials, carbon nanotubes (CNTs) and graphene have recently been subjects of interest due to their favorable properties to perform membrane structural enhancements related to surface charge, porosity, and mechanical stability. Therefore, studies on CNTs and graphene impregnated PES membranes have been intensified [3, 9, 15, 16–18].

[1]Dr. Jono Suhartono, Dr. Dyah Setyo Pertiwi, Carlina Noersalim, Devi Yulianingsih, Falashiva Sofianti
jono_suhartono@itenas.ac.id
Department of Chemical Engineering, Institut Teknologi Nasional (ITENAS), Jl. PHH. Mustafa No. 23, Bandung, Indonesia, 40124.

[2]Dr. Agus Saptoro
Department of Chemical Engineering, Curtin University Malaysia, CDT 250, Miri, 98009, Sarawak, Malaysia.

[3]Achmad Chafidz
Chemical Engineering Department, Universitas Islam Indonesia, Yogyakarta, 55584, Indonesia.

Unfunctionalized and functionalized carbon-based nanomaterials were found to strongly dictate the characteristics and performances of blended membranes [1, 4, 15, 16–22]. Furthermore, different treatments during membrane fabrication, e.g., air exposure, have also been identified to influence the membrane properties and flux capabilities [23, 24]. Despite extensive publications on incorporation of CNTs and graphene in PES membranes are available in the literature, little attention has been directed toward comparative performances of pristine CNTs (CNTs-P), oxidized CNTs (CNTs-O), pristine graphene nanoplatelets (GNPs-P), and oxidized graphene nanoplatelets (GNPs-) impregnated PES membranes under different air exposures.

In this study, the simultaneous effects of different carbon-based nanoparticles and air exposure on the blended membrane characteristics and performances are investigated. Parameters affecting these characteristics and performances of membranes fabricated using immersion precipitation (phase inversion) technique are also evaluated and discussed.

2 Methods

The fabrication of PES/carbon-based nanomaterial membranes involved three main steps: nanomaterial dispersion in N,N-dimethylformamide (DMF), homogenization of polymer/nanomaterial matrix solution, and phase inversion through immersion precipitation method. The polymer PES Ultrason® E6020P was obtained from BASF, Germany. DMF, GNPs-O, and GNPs-P were purchased from Sigma Aldrich, Singapore, and CNTs-O and CNTs-P from Haydale, Inc, UK. Other chemicals such as sodium hydroxide or hydrochloric acid were bought from Brataco Chemicals, Indonesia.

2.1 Dispersion of Nanomaterials

The dispersed nanomaterials were prepared by mixing 0.0567 g of nanomaterial and 100 mL DMF in a volumetric flask. The mixture was then shaken for 1 min to disperse the nanomaterials. To further homogenize the dispersion, the flask was placed in the ultrasonic bath (Digital Ultrasonic Cleaner 303363, Krisbow, China). Ultrasonification was carried out within 1 h, divided into four repeated procedures. Each procedure consisted of ultrasound irradiation at 30 kHz frequency for 15 min and cooling down the nanoparticle-dispersed solution for 5 min. The same procedure was repeated four times; therefore, the total duration of ultrasonification was 60 min. The water bath temperature was kept below 37 °C by adding fresh deionized water. This cooling aims to prevent overheating due to the ultrasonification process.

2.2 PES/Nanomaterials Composite Membrane Synthesis

An amount of 30 mL of dispersed nanomaterials was added to a beaker glass containing 5.67 g of PES powder. To ensure the homogeneity of the mixture, it was then stirred by a mechanical agitator at 250 rpm for 3 h at 70 °C. A water bath was used to maintain the desired temperature. Once a homogeneous mixture was obtained, the solution was stored in a desiccator to minimize air contact. The solution was then cooled in a water bath containing ice water until the temperature dropped to 22 ± 1 °C. Afterward, the solution was casted on a glass plate after the solution was without bubbles. The casting process was done in a 30 · 35 cm flat glass using a casting knife (Doctor's Blade method) to have a desirable thickness of ± 200 mm. For each nanomaterial incorporated PES membrane, two types of casted solutions were prepared: a casted solution having no contact with air (0 s) and a casted solution exposed to air with a humidity of 60 % for 60 s. These casted solutions were then immersed in a coagulation bath containing deionized water. The immersed membrane was kept inside the coagulation bath for 2 h to facilitate perfect transformation of the membrane.

2.3 Membrane Characterization

2.3.1 Membrane Porosity

Porosity is defined as the pore volume divided by the total volume of the membrane. Porosity is determined by the gravimetric method, in which the dry and wet membrane period was measured to estimate the amount of liquid present in the membrane [25, 26]. Porosity was then calculated by Eq. (1):

$$\varepsilon = \frac{m_l/\rho_l}{m_l/\rho_l + m_m/\rho_m} \cdot 100\% \quad (1)$$

where ε is the membrane porosity, m is the mass of the liquid (l) or membrane (m) in gram (g), and ρ is the density in g mL^{-1}.

2.3.2 Permeability

Permeability is the ability of a membrane to let water or liquid passing through its cross-sectional area. Permeability was obtained by measuring the value of flux or rate of permeation under a specied applied pressure. The permeability was defined as the flux difference at various pressure [27].

$$J = \frac{1}{A}\frac{dV}{dt} \quad (2)$$

where J is the membrane flux (L m^{-2}h^{-1}), V is the membrane permeate volume (L), A is the membrane surface area (m^2), and t is the operation time (h).

2.3.3 Contact Angle

The contact angle was predicted to determine the hydrophobicity or hydrophilicity characteristic of the synthesized membrane. Wettability of the membrane was measured using DAT 1100 (Fibro System ab, Sweden). As a wetting agent, 4 mL deionized water was employed, and the contact angle was measured at 12 s after the wetting fluid dropped on the membrane. A mean value from five replicates was adopted as a measured value.

2.3.4 Membrane Morphology

Morphological structures of the membrane were performed using scanning electron microscopy (SEM; Jeol JSM 6360, USA). The membrane was cracked by liquid nitrogen-assisted freeze-fracturing method and coated using a gold sputtering machine to obtain 3 nm thickness of the coating layer. The membrane was then placed inside the vacuum chamber. The SEM beam was focused into a targetted point on the sample and high electron energy scanned the sample resulting in two- or three-dimensional image resolutions. This image was generated from a pattern representing interactions between the electrons and atoms inside the sample.

2.3.5 Tensile Strength

The tensile strength test is a method adopted to examine the strength of a material by applying an axial force load. The tensile strength test was conducted to estimate the strength of the fabricated membrane against the applied pressure. The PES membrane was formed into a rectangle shape with the dimension of 40 ·2 mm. The tensile force was applied from the bottom upward to the membrane layer clasped on its both sides in the clamping system. PES membranes with and without addition of nanomaterial and with 0 s and 60 s air exposure were tested to obtain the stress-strain and Young's modulus characteristics, voltages at their peak points, and elongations at their break points.

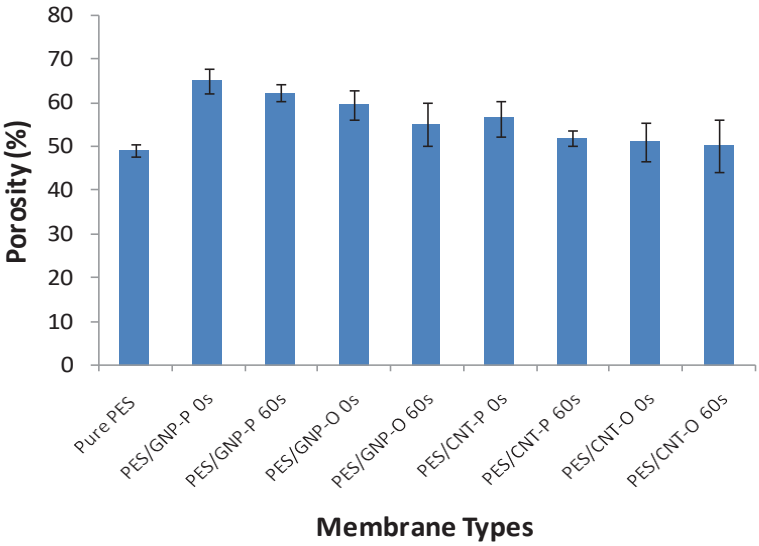

Figure 1. Porosity of PES membrane with and without impregnation of carbon-based nanomaterials.

3 Results and Discussion

3.1 Porosity

Impregnated membranes possess higher porosities compared to pure PES membranes as illustrated in Fig. 1. A pure PES membrane has a porosity of 49.17 %, and impregnations of carbon-based nanomaterials resulted in increasing porosities up to 32 %. The highest membrane porosity of 65 % was obtained when GNP-P was incorporated into the PES membrane without air exposure. The platelet structure of GNPs forms more pores during membrane fabrication due to the high random plate position on the membrane compared to the one on the tube structure. Increasing membrane porosity is therefore affected by the higher number of pores in the membrane. The porosity itself is the proportion of void space which can be occupied by water or air. Greater membrane porosity enables a higher volume of fluid to fill in the membrane.

Fig. 1 also indicates that membrane fabrication involving air exposure resulted in lower membrane porosity as compared to membrane fabrication without any air exposure. In this study, 60 s air exposure provided sufficient evaporation time for the DMF solvent from the membrane surface. Consequently, this delayed the membrane solidification process, thereby producing smaller membrane surface pores and subsequently lower porosity of the membrane.

From this figure it is also evident that oxidized carbon-based nanomaterials either with 0 s or 60 s air exposure possess higher porosities compared to pristine carbon-based nanomaterials. The presence of oxidized functional groups in the carbon-based nanomaterials provides more charges in the membrane, and these charges promote the membrane electronegativity as reported by earlier studies [18, 28, 29]. Increasing electronegativity induces carbon-based nanomaterial polarity and enhances the homogeneity in the polar DMF solvent. Hence, oxidized carbon-based nanomaterials are attributed to lower porosity compared to their pristine counterparts due to their homogeneous distribution in the solvent and polymer solution.

3.2 Contact Angle

Pure PES membranes are hydrophobic which tend to have high fouling propensity during their operation. Thus, it is desirable to synthesize a membrane having more hydrophilic properties. Measurement of contact angle (CA), often also named angular contact, was performed to evaluate hydrophilicity or hydrophobicity of the membrane surface. The contact angles of the PES membranes with and without the addition of carbon-based nanomaterials are presented in Fig. 2. It is apparent that nanomaterial-impregnated PES membranes have significantly lower membrane contact angles than pure PES membranes. PES materials are originally hydrophobic. However, during membrane preparation, the PES polymer was in contact with the polar DMF solvent. As a result, this polar solvent may diminish the hydrophobic properties of the PES polymer.

In this work, it was also found that all fabricated membranes have contact angles less than 90°. As reported by Yuan and

Lee [30], a contact angle of less than 90° indicates favorable surface wetting and the fluid is distributed to a large area on the surface. In contrast, contact angles above 90° generally points to unfavorable surface wetting. Under this scenario, the fluid has minimum contact with the surface and tends to form a compact liquid droplet. Therefore, the membrane is considered to be hydrophilic when it has contact angles greater than 0° and below 90°. On the other hand, contact angles more than 90° stipulate the hydrophobic characteristic. Accordingly, all membranes synthesized in this study can be categorized as hydrophilic membranes.

Pristine carbon-based nanomaterials tend to have hydrophobic properties. Consequently, contact angles of pristine carbon-based nanomaterials incorporated membranes were higher. Nevertheless, as displayed in Fig. 1, the increasing porosity may affect the ability of the membrane to adsorb water and thus decrease its hydrophobic properties. Fig. 2 also revealed that smaller contact angles could be obtained by oxidizing carbon-based nanomaterials and these phenomena are consistent either for GNPs or CNTs. The existence of oxidized functional groups on carbon-based nanomaterials stimulates the reduction of hydrophobicity of nanomaterials themselves [31]. Consequently, the addition of oxidized nanomaterials increases the membrane hydrophilicity as indicated by the lower contact angle.

Fig. 2 demonstrates that almost all impregnated carbon-based nanomaterial membranes have smaller water contact angles compared to the pure PES membrane. However, the water contact angle of the PES/GNP-P membrane without air exposure is slightly larger compared to the pure PES membrane, i.e., 77.35° to 76.14°, respectively. The incorporated GNPs at low loading of 0.3 % resulted in higher membrane surface roughness but produced well-distributed GNPs particles [34]. Therefore, although the increase of surface roughness would reduce the contact angle, the PES/GNPs-P membrane still has a larger contact angle than the PES membrane due to the well-distributed GNPs in the membrane which are naturally hydrophobic.

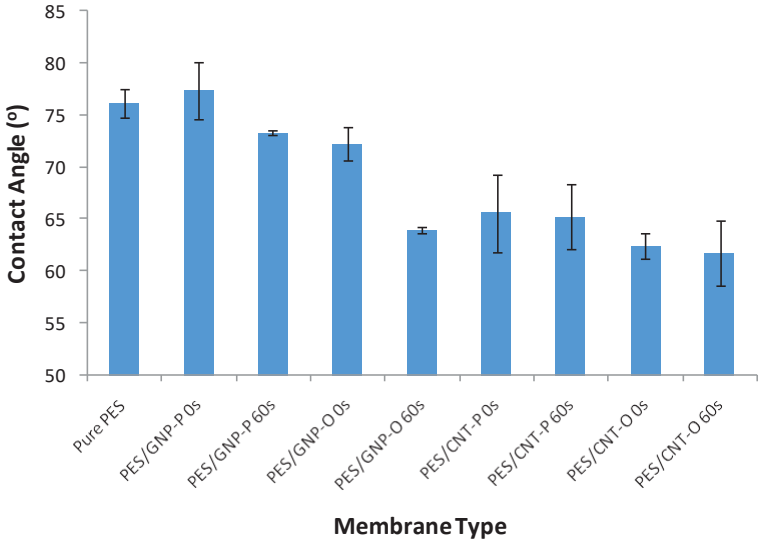

Figure 2. Contact angle measurement of the PES membrane impregnated with carbon-based material in comparison to the pure PES.

Meanwhile, the contact angle of the PES/CNTs-P membrane was found to be smaller than that of the PES membrane. This might be due to more CNT agglomerates formed in the polymeric membrane compared to GNPs as reported by Yue et al. [35]. The agglomeration might hinder the reactivity of CNTs and ability to improve the membrane hydrophobicity [34].

3.3 Morphological Characteristics

Images of the fabricated membrane generated by SEM at a magnification of 1000· are displayed in Fig. 3. The membrane pores showed a sponge-like structure consisting of small pores and large channeling pores.

There are several influencing factors affecting the membrane morphology of the synthesized membrane via phase inversion. Structure, porosity, and selectivity of the fabricated membrane can be controlled by regulating polymer solution composition, types of solvent and non-solvent, polymer concentration, liquid composition in the coagulation bath, casting solution composition, and operating conditions during fabrication. According to Mulder [27], there are two possible mechanisms associated with membrane morphology formation. When the membrane structure is formed as soon as the film layer is immersed in the gelatinization medium, morphology formation follows an instantaneous demixing mechanism. On the contrary, delayed demixing involves a waiting period before the membrane structure starts to configure.

The formation of a finger-like structure on the membrane is hypothesized to be caused by the delayed solvent/non-solvent replacement during the coagulation process. This delay is a result of increasing viscosity due to the impregnated carbon-based nanomaterial [18]. The evaporation of air has an impact on the surface skin of the membrane in which delayed evaporation time resulted in smaller, denser, and smoother pore formation of the upper skin. These findings are in accordance to the study conducted by Kusworo et al. [32].

Although measurements of the pore size in the support membrane are doable, the pore sizes of the active layer possibly were not accurate. These demonstrate that either pure PES or PES/carbon-based nanomaterial membranes can be classified as asymmetric types. From Fig. 3 it is obvious that the membrane pores in the support layer were larger than those on the membrane surface layer. These pore size dissimilarities exist due to the differences between rates of solvent diffusion in the supporting and active layer. Membrane solidification took place from the edge to the center of the casting solution. Therefore, the liquid-liquid demixing of solvent and non-solvent firstly occurs at the top of the casting solution. The penetrating non-solvent then passed through the bottom of the membrane and left some non-solvent accumulated in the support layer to produce larger membrane pores.

The sizes of support membrane pores were estimated using SEM as presented in Tab. 1. Results in this table clearly unveil that PES/GNPs-O 60 s and PES/CNTs-O 60 s membranes have narrower pore

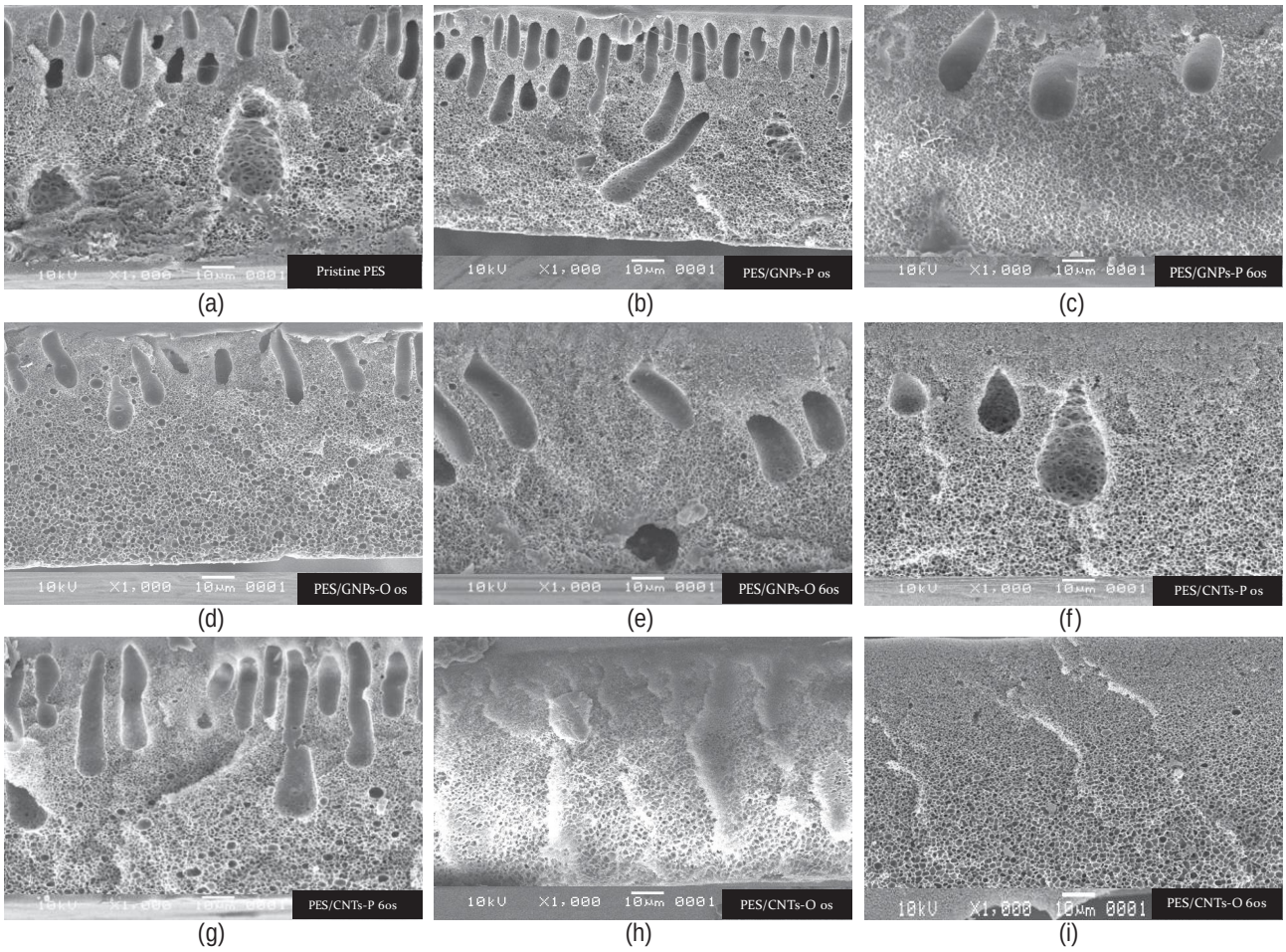

Figure 3. Images of fabricated membrane PES/carbon-based nanomaterials. (a) Pure PES 0 s, (b) PES/GNPs-P 0 s, (c) PES/GNPs-P 60 s, (d) PES/GNP-O 0 s, (e) PES/GNP-O 60 s, (f) PES/CNT-P 0 s, (g) PES/CNT-P 60 s, (h) PES/CNT-O 0 s, (i) PES/CNT-O 60 s.

Table 1. Range of pore size of fabricated membrane support.

Membrane	Air exposure [s]	Pore size range [mm]
Pure PES	0	0.53–2.12
PES/GNPs-P	0	0.35–2.39
PES/GNPs-P	60	0.50–1.15
PES/GNPs-O	0	0.44–1.41
PES/GNPs-O	60	0.35–0.73
PES/CNTs-P	0	0.39–1.41
PES/CNTs-P	60	0.54–1.25
PES/CNTs-O	0	0.53–1.07
PES/CNTs-O	60	0.67–0.88

size ranges due to the existence of oxidized functional groups coupled with delayed membrane coagulation. The incorporations of oxidized functional groups in the mixed matrix PES/carbon-based nanomaterial improved the homogeneity of the nanomaterial in the casting solution. Thus, they created a more compact and smaller pore size than of the ones possessed by non-oxidized functional groups impregnated PES membranes. In addition, 60 s air exposure provides an extra time for the solvent to pre-evaporate and strengthen the polymer-polymer integration.

3.4 Permeability

Fig. 4 illustrates that longer air evaporation resulted in a slight decrease of the water permeability for almost all fabricated membranes. This reduction is attributable to the delayed solvent/non-solvent demixing process which caused more dense membrane on the membrane active surface. The evaporation time promotes a rising polymer concentration at the top of the membrane layer, thus effectuating a smaller or dense pore membrane. This layer also suppresses the exchange rate of residual solvent and non-solvent through the membrane surface during the demixing process at the coagulation bath. This phenomenon created the formation of a membrane having smaller pore sizes, thus leading to lower fluxes.

Fig. 4 also displays a comparative analysis of permeabilities of pure PES and blended PES and nanomaterials. The addition

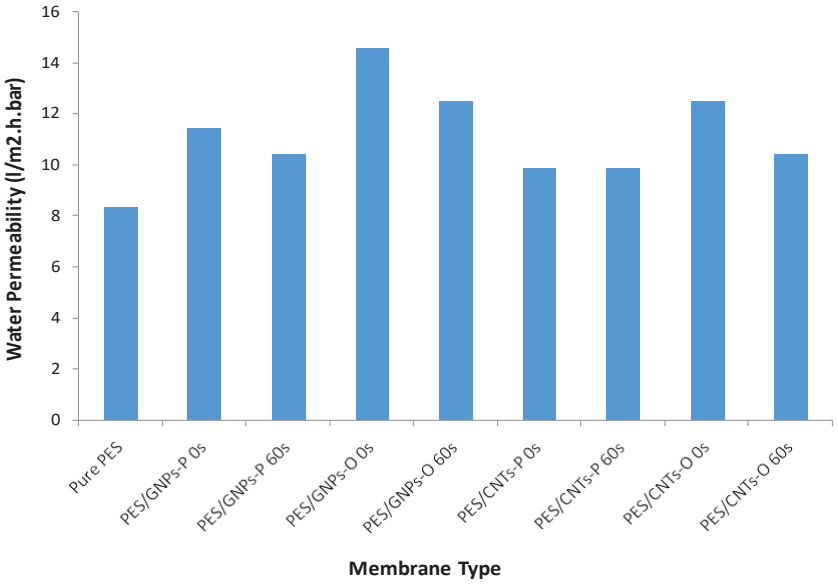

Figure 4. Water permeability of fabricated PES/carbon-based nanomaterial membranes in comparison to the pure PES membrane.

of carbon-based nanomaterials resulted in a higher permeability compared to the pure PES membrane. This is consistent with findings in Sect. 3.1 where PES/carbon-based nanomaterial membranes own higher porosities than the pure PES membrane. Referring to Van Der Bruggen et al. [33], since their permeability range is from 8 to 15 L $m^{-2}h^{-1}bar^{-1}$, all synthesized membranes in this study can be categorized as nanofiltration or tight ultrafiltration membrane.

The PES/GNPs-O membrane provided the highest permeability (Fig. 4) and smaller support pore size (Tab. 1) which demonstrates that the membrane may have higher permeation flux and rejection to the undesired solute compared to the other membranes. Moreover, this membrane also has a small contact angle (Fig. 2) which indicates its more hydrophilic properties and high fouling resistance.

The fabrication of the PES/GNPs-O membrane could be done by simple phase inversion method through immersion precipitation route making this method the most widely used for commercial membrane fabrication today. For instance, studies of the application of this membrane type have been conducted in water treatment [36–39], ethanol dehydration [40], or gas separation [41]. However, understanding the properties and characters would promote the decision for its technological application in order to obtain an effective and efficient process.

3.5 Mechanical Properties

The maximum stress of the fabricated membrane was described by the tensile test and Young's modulus as summarized in Figs. 5 and 6.

Fig. 5 illustrates that all impregnated membranes at 0 s air exposure have a higher stress at the break compared to the pure PES membrane. On the other hand, 60 s air exposure slightly diminished the stress at the break of the membrane. The impregnation of nanomaterials also produced a higher

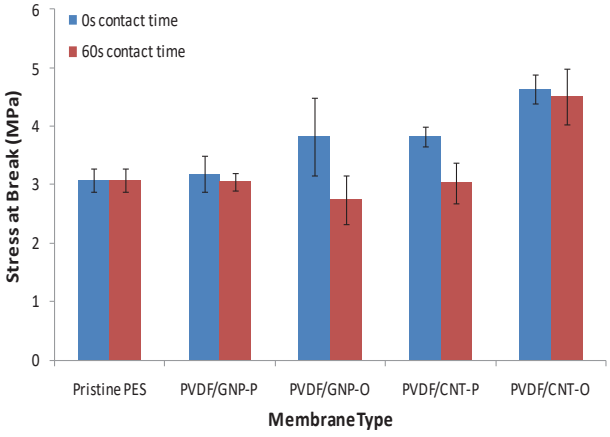

Figure 5. Stress at the break of PES/carbon-based nanomaterial in comparison to pristine PES.

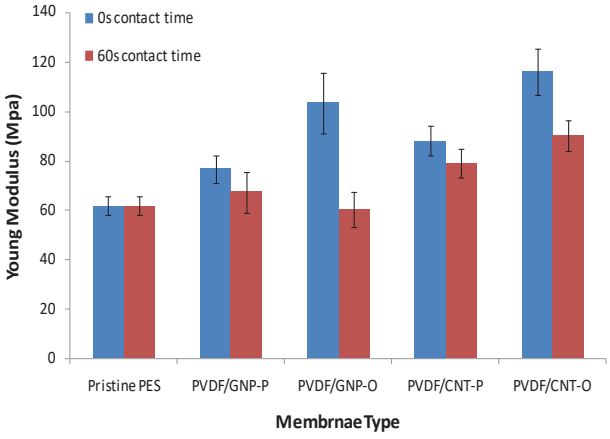

Figure 6. Young's modulus of PES/carbon-based nanomaterial in comparison to pristine PES.

Young's modulus than of the pristine PES membrane. Fig. 5 indicates that the stress at the break of pristine PES was 3.08 MPa. The addition of carbon-based nanomaterial enhanced the membrane stress at the break up to 4.64 MPa. Young's modulus of the pristine PES membrane was 61.6 MPa, while that of the PES/carbon-based nanomaterial significantly increased up to 115 MPa. This indicates that incorporating either GNP or CNT to the PES membrane resulted not only in improved strength but also in a more rigid or inelastic membrane.

4 Conclusions

The characteristics of pure PES and blended carbon-based nanomaterial and PES membranes were investigated at different air exposures during fabrication. The impregnation of carbon-based nanomaterials increased membrane porosity and permeability up to 30 % and 88 %, respectively, compared to the ones associated with the pure PES membrane. On the other hand, membrane contact angles were significantly lower by incorporation of oxidized functional groups, indicating that that the membrane possesses hydrophilic properties. The fabricated membrane has a sponge-like structure comprising small pores and large channeling pores.

Based on their measured water permeabilities in the range of 8–15 L $m^{-2}h^{-1}bar^{-1}$, the synthesized membranes can be categorized as nanofiltration or tight ultrafiltration membranes. A membrane exposed to air for 60 s during its fabrication exhibits a denser pore size than without air exposure. Compared to the GNPs nanomaterial incorporated PES membrane, the CNTs impregnated PES membrane has a lower porosity, contact angle, and permeability. It is also evident that the addition of carbon-based nanomaterials into the PES membrane reduce the membrane elasticity and on the contrary increase the strength of the membrane.

Acknowledgment

The first five authors acknowledge the Ministry of Research and Higher Education, Indonesia, and the Institut Teknologi Nasional (Itenas) Bandung, Indonesia, for their financial support through research grant No. 292/B.05/LPPM-Itenas/III/2019. A. Saptoro is grateful to Curtin University Malaysia's Strategic Research Incentives Scheme Cost Center: 4830/A14.

The authors have declared no conflict of interest.

Abbreviations

CA	contact angle
CNTs	carbon nanotubes
DMF	dimethylformamide
GNPs	graphene nanoplatelets
-O	oxidized
-P	pristine
PES	polyethersulfone
SEM	scanning electron microscopy

